ORIGINAL ARTICLE

A C G publications

Rec. Nat. Prod. 18:1 (2024) 95-106

records of natural products

Anthraquinones and Macrocyclic Lactones from Endophytic Fungus *Penicillium roseopurpureum* and Their Bioactivities

Berivan Dizmen [1], Göklem Üner [2], Melis Küçüksolak [2], Ahmet C. Gören [3], Petek Ballar Kırmızıbayrak [4] and Erdal Bedir [2*]

[1]*Department of Biotechnology and Bioengineering, İzmir Institute of Technology, 35430, Urla, İzmir, Türkiye*

[2]*Department of Bioengineering, Faculty of Engineering, İzmir Institute of Technology, 35430, Urla, İzmir, Türkiye*

[3]*Department of Chemistry, Faculty of Science, Gebze Technical University, 41400, Gebze, Kocaeli, Türkiye*

[4]*Department of Biochemistry, Faculty of Pharmacy, Ege University, 35100, Bornova, İzmir, Türkiye*

(Received September 07, 2023; Revised October 26, 2023; Accepted November 17, 2023)

Abstract: Endophytic fungi colonize the internal and distinct tissues of the host plants. In recent years, there has been growing interest in endophytic fungi as valuable sources for drug discovery based on their rich metabolic profiles consisting of novel and bioactive compounds. Accordingly, our preliminary study demonstrated that an endophyte, namely *Penicillium roseopurpureum* isolated from *Astragalus angustifolius*, had high chemical diversity with an antiproliferative effect. Herein, fermentation of *P. roseopurpureum* resulted in the production of five new anthraquinone-type compounds (**2**, **4**, **6**, **7**, **8**) together with several known compounds [11-methoxycurvularin (**1**: epimeric mixture of **1a** and **1b**), carviolin (**3**), 11-hydroxycurvularin (**5**: diastereoisomeric mixture of **5a** and **5b**) and 1-*O*-methylemodin (**9**)]. The structures of the new compounds were established by NMR spectroscopy and HR-MS analysis. Cytotoxicity studies demonstrated that none of the compounds except for **1** and **5** had antiproliferative activity against prostate cancer cell lines. Interestingly, **1** was found as cytotoxic, whereas **5** exhibited cytostatic properties. Also, 7-AAD/Annexin V staining supported these results by showing that **1** caused cellular death, while **5** did not show any increase in dead cell content in comparison to the control. Lastly, cell cycle analysis showed that compounds had distinctive cell cycle arrest patterns.

Keywords: Endophytic fungi; natural products; anthraquinones; Macrocyclic Lactones; cytotoxicity; cell cycle Arrest.

1. Introduction

Endophytic fungi are fungal communities living in the tissues of living plants without causing visible damage. These microorganisms colonize in various organs of host plants, including the root, stem, leaf, flower, fruit, and seed, predominantly in intercellular or intracellular spaces [1, 2]. The interaction between the host plant and endophytic fungi is mutually beneficial to both parties.

* Corresponding author: E-Mail: erdalbedir@iyte.edu.tr
These authors contributed equally: Berivan Dizmen, Göklem Üner, Melis Küçüksolak.

The article was published by ACG Publications
http://www.acgpubs.org/journal/records-of-natural-products January-February 2024 EISSN:1307-6167
DOI: http://doi.org/10.25135/rnp.426.2309.2896
Available online: January 01, 2024

Endophytes produce a diverse range of natural products that are beneficial to the plant, with low toxicity, protecting and promoting survival conditions for the host plant while creating a selective environment for various microorganisms. In this relationship, endophytes must continuously respond to the defense mechanisms of the host plant. This creates a selection pressure that drives the development of new metabolic pathways [3–5].

The field of endophytic fungi remains largely unexplored, yet it holds promise as a potential source of new and valuable natural products for use in medicine, agriculture, and industry. Endophytic fungi produce various secondary metabolites such as steroids, alkaloids, phenols, isocoumarins, xanthones, quinones, and terpenoids [6, 7]. Several studies have discovered new bioactive compounds that offer significant health benefits. These compounds possess various biological properties, including antibacterial, antifungal, anti-inflammatory, antiprotozoal, insecticidal, immunomodulatory, antiviral, and cytotoxic activities [8, 9]. A previous study reported that 51% of biologically active compounds derived from endophytic fungi were previously unknown compounds [10]. Therefore, these resources are valuable for discovering new and potent bioactive compounds. In addition, a semi-synthetic derivative of enfumafungin, which is an antifungal triterpenoid originating from the endophytic fungus *Hormonema* sp., was approved by the FDA in 2021, revealing the importance of this group of organisms [11–13].

During our preliminary study, *Penicillium roseopurpureum* 1E4BS1, isolated from *Astragalus angustifolius*, was found to be chemically diverse and had meaningful cytotoxic activity. Herein, based on the potential of endophytic fungi in drug discovery studies, we aimed to obtain secondary metabolites of *P. roseopurpureum* and determine their cytotoxic activities.

2. Materials and Methods

2.1. Microorganism

The endophytic fungus *Penicillium roseopurpureum* 1E4BS1 was isolated from *Astragalus angustifolius* collected in Manisa-Spil Mountain, İzmir, Turkey, in June 2013. The isolate was authenticated by molecular identification based on rDNA ITS sequence analysis. The ITS region was sequenced using primers ITS437 and ITS1F. The assembled DNA sequences were compared with those in GenBank and MycoID databases (Genbank accession number: KJ775658.1). The original culture was deposited at the Bedir Laboratory with the deposit number 20131E4BS1 [14]. The strain was maintained on potato dextrose agar (PDA) slants and stored at 4 °C.

2.2. Fermentation and Isolation

The fungus was pre-cultivated on PDA for ten days at 25 °C. The spore solution was prepared with 0.1% (v/v) Tween 80 and used to inoculate (2% v/v) five of 5 L flasks containing 2 L potato dextrose broth (PDB). Fermentation was performed in a rotary shaker at 180 rpm, 25 ºC for 20 days. Every seven days, samples with a volume of 10 mL were taken and centrifuged. The supernatants were extracted with EtOAc to profile the metabolite diversity of the fungus.

Isolation studies on the EtOAc extract (599.8 mg) started with a 135 g silica gel using open-column chromatography. First, the extract was dissolved in $CHCl_3$:MeOH mixture, impregnated with silica gel, and dried. Subsequently, the dried silica containing the extract was applied to the silica column equilibrated with $CHCl_3$. The column was eluted with $CHCl_3$:MeOH (100:0→0:100). Collected fractions showing similar profiles were pooled together, and 22 main fractions were obtained.

Among these 22 main fractions, seven of them were selected for further isolation and purification studies according to TLC profiles. Detailed isolation procedures were given in below.

S4-14 (83 mg) was chromatographed over RP-C18 column (30 g) and eluted with MeOH:H_2O (50:50 → 100:0) solvent system and sixteen subfractions were obtained. S4-14_RP7-12 (32.8 mg) subfraction was subjected to a silica gel column (10 g) and eluted with $CHCI_3$:MeOH (99:1→0:100) solvent system. S4-14_RP7-12 column gave **1** (8.3 mg), and S4-14_RP7-12_S71-86 subfraction was further subjected to a RP-C18 column (20 g) and eluted with MeOH:H_2O (55:45) solvent system to give **2** (4.7 mg).

S24-44 (104.4 mg) was chromatographed over a silica gel column (80 g) using *n*-Hex:EtOAc:MeOH (10:10:0.5 → 100% MeOH) solvent system, and 23 subfractions were obtained. S24-44_S145-181 (31 mg) subfraction was further subjected to a Sephadex LH-20 column (15 g) and eluted with MeOH (100%) as mobile phase to give **3** (10 mg) and **4** (2.4 mg). S24-44_S145-181_Sep15-19 and S24-44_S145-181_Sep22-34 subfractions were combined and subjected to a Sephadex LH-20 column (15 g) using MeOH (100%) as mobile phase, which afforded **3** (11.2 mg) and **4** (3.9 mg).

S65-90 (87.9 mg), one of the main fractions, was chromatographed over Sephadex LH-20 column (35 g) and eluted with MeOH (100%) as mobile phase, and nine subfractions were obtained. S65-90_Sep12-15 (6.5 mg) subfraction was further subjected to a silica gel column (10 g) using *n*-Hex:EtOAc:MeOH (10:10:0.5→100% MeOH) as mobile phase to give **5** (4.2 mg).

S107-131 (58.8 mg) was chromatographed over Sephadex LH-20 column (35 g) and eluted with MeOH (100%) as mobile phase, and eight subfractions were obtained. S107-131_Sep41-52 (7 mg) subfraction was subjected to Sephadex LH-20 column (15 g) using MeOH (100%) as mobile phase, and four subfractions were obtained. S107-131_Sep53 (2.7) and S107-131_Sep41-52_Sep28-43 (1.7 mg) subfractions were combined to give **6** (4.4 mg).

S170-171 (93.5 mg) was chromatographed over Sephadex LH-20 column (15 g) and eluted with MeOH (100%) as mobile phase, and ten subfractions were obtained. S170-171_Sep36-48 (12.6 mg) subfraction was subjected to a silica gel column (10 g) using $CHCI_3$:MeOH (90:10→0:100) solvent system, and six subfractions were obtained. S170-171_Sep36-48_S27 (10 mg) subfraction was subjected to a silica gel column (10 g) and eluted with *n*-Hex:EtOAc:MeOH (10:10:4→100% MeOH) solvent system to give **7** (3.8 mg) and **8** (2.5 mg).

S15-23 (43.8 mg) was chromatographed over Sephadex LH-20 column (30 g) and eluted with MeOH (100%) as mobile phase, and ten subfractions were obtained. S15-23_Sep7-21 (14.5 mg) subfraction was subjected to Prep TLC (RP-C18) with MeOH:H_2O (85:15) solvent system. S15-23_Sep7-21_Prep1 was further subjected to Sephadex LH-20 column (10 g) and eluted with MeOH (100%) as mobile phase to afford **9** (1.7 mg).

2.3. Cytotoxicity

Cell viability was determined using the MTT assay. After cells were treated with various concentrations of compounds/extract or vehicle for 48 h, cells were incubated with 5 mg/mL MTT (3-(4,5- Dimethyl-2-thiazolyl)-2,5-diphenyl-2H-tetrazolium bromide) (Sigma Aldrich, UK). Following 4 h incubation at 37 °C and 5% CO_2, absorbance was measured by using a microplate reader at 590 nm (Varioscan, Thermo Fisher Scientific, US). Graph Pad Prism 6 (San Diego, CA, US.) was used to calculate the IC_{50} values.

2.4. Detection of Cell Death Ratio

FITC Annexin V Apoptosis Detection Kit with 7-AAD (BioLegend Inc) was used to detect cell death morphology. After 48 h incubation with compounds or vehicle, cells were suspended in 100µL of Annexin V binding buffer, and then 5 µL of FITC-conjugated Annexin V and 7-AAD were added to samples. Following the incubation at room temperature for 15 min in the dark, the stained cells were examined using a FacsCanto Flow Cytometry (BD Bioscience, US).

2.5. Detection of Cell Cycle

Propidium Iodide (PI)/RNase Staining Solution (Cell Signaling) was used to investigate the effect of compounds on the cell cycle. After LNCaP cells were treated with compounds or vehicle, cells were fixed in cold 70% ethanol for 30 min on ice. After centrifugation, cell pellets were suspended in 0.1% Triton X solution and incubated for 5 min. Then cells were centrifugated, and pellets were suspended in 400 µl PI/RNAase solution. After 15 min incubation at room temperature, cells were analyzed by FacsCanto Flow Cytometry (BD Bioscience, US).

3. Results and Discussion

After extracting the fermentation broth of *Penicillium roseopurpureum* 1E4BS1 with EtOAc, several metabolites were purified using column chromatography methods, as described in the methods section. Spectral data inspection (MS, 1D-, and 2D-NMR) led to the structural determination of five new compounds (Figure 1). The known compounds were identified based on a comparison of their previously reported spectra: 11-methoxycurvularin (epimeric mixture; **1**) (Figure S1-7 and Table S1) [15–17], carviolin (**3**) (Figure S15-21 and Table S2) [18, 19], 11-hydroxycurvularin (diastereoisomeric mixture; **5**) (Figure S29-35 and Table S3) [20], and 1-*O*-methylemodin (**9**) (Figure S57-63 and Table S4) [21]. The structure elucidation of five new compounds is discussed below.

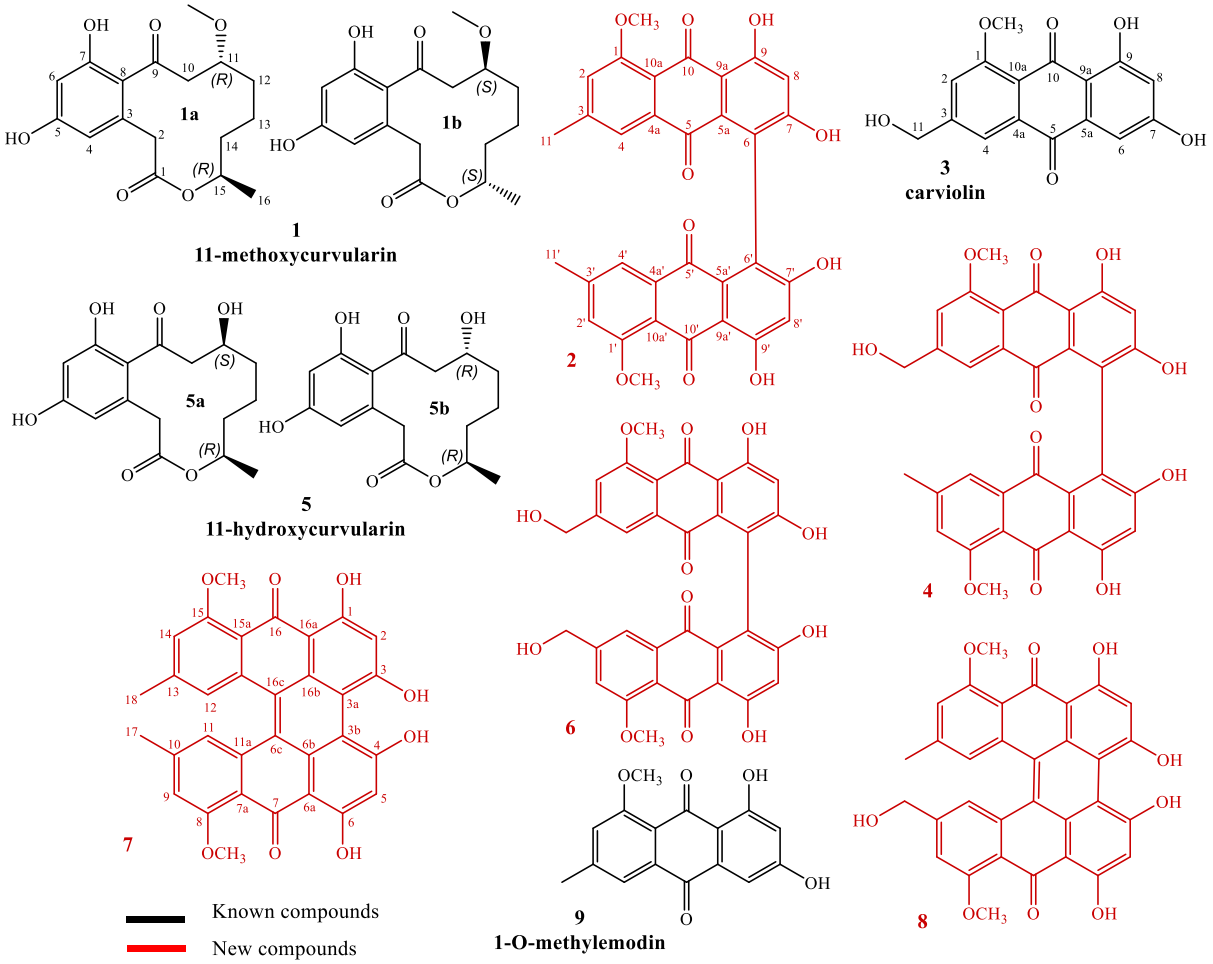

Figure 1. Structure of metabolites (**1-9**)

3.1. Structure Elucidation

The HR-ESI-MS spectrum of **2** exhibited a major ion peak at *m/z* 567.1279 $[M+H]^+$ (calcd. 567.1291) supported a molecular formula $C_{32}H_{22}O_{10}$ with twenty-two indices of hydrogen deficiency (Figure S8-14). Analysis of its ^{1}H- and ^{13}C-NMR spectra revealed the presence of a methyl ($\delta_{H\text{-}11}$, 2.32 s, $\delta_{C\text{-}11}$ 21.5 q), a methoxy group (H-1-OMe: δ 3.91 s; C-1-OMe δ 56.3 s), three aromatic carbon methines ($\delta_{C\text{-}2}$ 118.5, $\delta_{C\text{-}4}$ 119.6, $\delta_{C\text{-}8}$ 107.1), and ten non-protonated carbons (six aromatic $\delta_{C\text{-}1}$ 159.6, $\delta_{C\text{-}3}$ 144.9, $\delta_{C\text{-}4a}$ 135.8 s, $\delta_{C\text{-}5a}$ 131.9 s, $\delta_{C\text{-}6}$ 127.0, $\delta_{C\text{-}7}$ 159.6, $\delta_{C\text{-}9}$ 164.8, $\delta_{C\text{-}9a}$ 106.8 s, $\delta_{C\text{-}10a}$ 118.4 s and two keto carbons at $\delta_{C\text{-}5}$ 184.2 s, $\delta_{C\text{-}10}$ 207.3 s). Detailed inspection of the 1D-, 2D-NMR and HR-ESI-MS

spectra implied that **2** was a homodimeric anthraquinone, suggested to be linked through C-6 and C-6' carbons. Additionally, the monomeric unit was established as 1-*O*-methylemodin by comparing the spectral data with those of the previous report [21]. In the ^{1}H- NMR spectrum of **2**, the aromatic proton was lacking for C-6 when compared to that of 1-*O*-methylemodin [21], which substantiated that the monomers were coupled to each other at C-6 and C-6'. Although a circular dichroism (CD) experiment was performed, it was inconclusive, and we were unable to establish the atropisomerism at C-6/C-6' (Sa or Ra) for this bis-anthraquinone structure. Thus, based on the data from ^{1}H- and ^{13}C-NMR and 2D spectra (COSY, HSQC, and HMBC), the planar structure of **2** was determined to be 2,2',4,4'-tetrahydroxy-5,5'-dimethoxy-7,7'-dimethyl-[1,1'-bianthracene]-9,9',10,10'-tetraone (IUPAC name), a new natural product (^{1}H NMR and ^{13}C-NMR data see Table 1).

The HR-ESI-MS spectrum of **4** exhibited a major ion peak at *m/z* 583.1230 $[M+H]^+$, (calcd. 583.1240) supported a molecular formula $C_{32}H_{22}O_{11}$ with twenty-two indices of hydrogen deficiency (Figure S22-28). The spectroscopic features suggested that **4** was a dimeric anthraquinone-like **2**. Compound **4** had a 16 amu (atomic mass unit) increase compared to **2**, implying oxygenation. In accordance, a primary alcohol group was readily assigned based on the resonances of δ 4.53 (s, 2H) and δ 62.3 in the ^{1}H- and ^{13}C-NMR spectrum of **4**, respectively. Detailed inspection of the 1D-, 2D-NMR and HR-ESI-MS spectra inferred that **4** was a heterodimer anthraquinone. One of the two monomeric units was established as 1-*O*-methylemodin by comparing the spectral data with those of the previous report, and **2** [21], and the other monomeric unit was established as carviolin by comparing the spectral data with those of previous reports and **3** [18, 19]. As in the case of **2**, in the ^{1}H NMR spectrum of **4**, the aromatic H-6 proton was missing in both 1-*O*-methylemodin and carviolin substructures [18, 19, 21], signifying that monomeric moieties were linked through C6/C6'. CD experiment was also unsuccessful in determining the absolute stereochemistry of **4**. Consequently, the planar structure of **4** was elucidated as 2,2',4,4'-tetrahydroxy-7-(hydroxymethyl)-5,5'-dimethoxy-7'-methyl-[1,1'-bianthracene]-9,9',10,10'-tetraone, a new heterodimeric anthraquinone. (^{1}H-NMR and ^{13}C-NMR data see Table 1).

The HR-ESI-MS spectrum of **6** exhibited an ion peak at *m/z* 599.1176 $[M+H]^+$ (calcd. 599.1189) supported a molecular formula $C_{32}H_{22}O_{12}$ with twenty-two indices of hydrogen deficiency (Figure S36-42). The spectroscopic features suggested that **6** was a dimeric anthraquinone like **4**. Compound **6** had a 16 amu increase compared to **4**, implying oxygenation. In accordance, two primary alcohol group was readily assigned based on the resonances observed at δ 4.53 (s, $H_{2\text{-}11}$, $H_{2\text{-}11'}$) and δ 62.2 in the ^{1}H- and ^{13}C NMR spectra of **6**, respectively. Detailed inspection of the 1D-, 2D NMR, and HR-ESI-MS spectra inferred that **6** was a homodimeric anthraquinone. The monomeric unit was established as carviolin by comparing the spectral data with those of previous reports and **3** [18, 19]. As in the case of **4**, compound **6** had a linkage through C6/C6' [18, 19, 21]. Consequently, the planar structure of **6** is 7,7'-diethyl-2,2',4,4',5,5'-hexamethyl-9,9',10,10'-tetramethylene-9,9',10,10'-tetrahydro-1,1'-bianthracene, yet determination of its stereo structure is warranted. A literature survey revealed that **6** was a new homodimeric anthraquinone. (^{1}H NMR and ^{13}C NMR data see Table 1).

The HR-ESI-MS spectrum of **7** exhibited a major ion peak at *m/z* 533.1246 $[M-H]^-$, (calcd. 533.1241) supported a molecular formula $C_{32}H_{22}O_8$ with six indices of hydrogen deficiency (Figure S43-49). The ^{1}H-NMR and ^{13}C-NMR spectra of **7** showed a close structural relationship with **2**. The spectroscopic features suggested that **7** was a naphtodianthrone derivative like **2**. Detailed inspection of the 1D-, 2D-NMR, and HR-ESI-MS spectra inferred that **7** was a homodimer naphtodianthrone. The monomeric unit was established as 1-*O*-methylemodin by comparing the spectral data with those of previous reports and **2** [21]. In the ^{1}H-NMR spectrum of **7**, the aromatic protons were lacking for C-6c, C-16c, C-3a, and C-3b when compared to that of 1-*O*-methylemodin [21], which substantiated that the substructures were connected through C-3a → C-3b and C-16c → C-6c bridges [18, 19, 21]. Consequently, the structure of 7 was elucidated as 1,3,4,6-tetrahydroxy-8,15-dimethoxy-10,13-dimethyldibenzo[a,o]perylene-7,16-dione, a new member of naphtodianthrone derivatives. (^{1}H-NMR and ^{13}C-NMR data see Table 2).

Table 1. NMR spectroscopic data for compounds **2**, **4** and **6** ([a]600 MHz and [b]500 MHz in DMSO-d_6)

	2[a]		**4**[a]		**6**[b]	
No	**δ_C, Type**	**δ_H (*J* in Hz)**	**δ_C, Type**	**δ_H (*J* in Hz)**	**δ_C, Type**	**δ_H (*J* in Hz)**
1	159.6 s	-	159.9 s	-	160.2 s	-
2	118.5 d	7.27 (s)	115.3 d	7.40 (s)	115.6 d	7.42 (s)
3	144.9 s	-	151.9 s	-	151.1 s	-
4	119.6 d	7.15 (s)	116.6 d	7.40 (s)	116.7 d	7.45 (s)
4a	135.8 s	-	135.6 s	-	135.4 s	-
5	184.2 s	-	ND	-	183.1 s	-
5a	131.9 s	-	131.2 s	-	130.9 s	-
6	127.0 s	-	ND	-	122.3 s	-
7	159.6 s	-	164.4 s	-	ND	-
8	107.1 d	6.15 (s)	107.3 d	6.39 (s)	107.5 d	6.63 (s)
9	164.8 s	-	164.4 s	-	164.0 s	-
9a	106.8 s	-	ND	-	109.9 s	-
10	207.3 s	-	180.1 s	-	186.2 s	-
10a	118.4 s	-	119.7 s	-	118.3 s	-
11	21.5 q	2.32 (3H, s)	62.3 t	4.53 (2H, s)	62.2 t	4.53 (2H, s)
1-OMe	56.3 q	3.91 (3H, s)	56.4 q	3.93 (3H, s)	56.4 q	3.88 (3H, s)
7-OH	-	ND	-	ND	-	10.82 (s)
9-OH	-	14.16 (s)	-	14.05 (s)	-	13.87 (s)
11-OH			-	5.45 (brs)	-	5.47 (brs)
1’	159.6 s	-	159.9 s	-	160.2 s	-
2’	118.5 d	7.27 (s)	118.8 d	7.31 (s)	115.6 d	7.42 (s)
3’	144.9 s	-	145.7 s	-	151.1 s	-
4’	119.6 d	7.15 (s)	119.8 d	7.26 (s)	116.7 d	7.45 (s)
4’a	135.9 s	-	135.6 s	-	135.4 s	-
5’	184.2 s	-	ND	-	183.1 s	-
5’a	131.9 s	-	131.2 s	-	130.9 s	-
6’	127.0 s	-	ND	-	122.3 s	-
7’	159.6 s	-	164.4 s	-	ND	-
8’	107.1 d	6.15 (s)	107.3 d	6.39 (s)	107.5 d	6.63 (s)
9’	165.0 s	-	164.4 s	-	164.0 s	-
9’a	106.8 s	-	ND	-	109.9 s	-
10’	207.3 s	-	180.1 s	-	186.2 s	-
10’a	118.4 s	-	118.9 s	-	118.3 s	-
11’	21.5 q	2.32 (3H, s)	21.5 q	2.34 (3H, s)	62.2 t	4.53 (2H, s)
1’-OMe	56.3 q	3.91 (3H, s)	56.4 q	3.93 (3H, s)	56.4 q	3.88 (3H, s)
7’-OH	-	ND	-	ND	-	10.82 (s)
9’-OH	-	14.16 (s)	-	14.05 (s)	-	13.87 (s)
11’-OH					-	5.47 (brs)

ND: Not determined.

The HR-ESI-MS spectrum of **8** exhibited a major ion peak at *m/z* 549.1196 $[M-H]^-$, (calcd. 549.1191) supported a molecular formula $C_{32}H_{22}O_9$ with 22 indices of hydrogen deficiency (Figure S50-56). The spectroscopic features suggested that **8** was a naphtodianthrone derivative like **7**. Compound **8** had a 16 amu (atomic mass unit) increase compared to **7**, implying hydroxylation. In accordance, a primary alcohol group was deduced based on the resonances of δ 4.25 (s, $H_{2\text{-}17}$) and δ 62.3, in the ^{1}H- and ^{13}C-NMR spectra of **8**, respectively. Detailed inspection of the 1D-, 2D-NMR, and HR-ESI-MS spectra inferred that **8** was a heterodimer naphtodianthrone. One of the two monomeric units was established as 1-*O*-methylemodin by comparing the spectral data with those of the previous report, and **2** [21], and the other monomeric unit was established as carviolin by comparing the spectral data with those of previous reports and **3** [18, 19]. As in the case of **3** and **2**, in the ^{1}H-NMR spectrum of **8**, the aromatic H16c/H6c and H3a/H3b protons were missing in both 1-*O*-methylemodin and carviolin substructures [18, 19, 21], signifying that the substructures were linked through two bridges: C16c → C6c and C3a → C3b. Consequently, the structure of **8** was elucidated as 1,3,4,6-tetrahydroxy-10-

(hydroxymethyl)-8,15-dimethoxy-13-methyldibenzo[a,o]perylene-7,16-dione. A literature survey revealed that **8** was a new heterodimeric naphtodianthrone. (^{1}H-NMR and ^{13}C-NMR data see Table 2).

Table 2. NMR spectroscopic data for compounds **7** and **8** (500 MHz in DMSO-d_6)

	7		**8**	
No	**δ_C, Type**	**δ_H (*J* in Hz)**	**δ_C, Type**	**δ_H (*J* in Hz)**
1	168.6 s	-	168.6 s	-
2	104.1 d	6.22 (s)	104.1 d	6.22^{z} (d)
3	172.1 s	-	172.0* s	-
3a	118.5 s	-	118.5 s	-
3b	118.5 s	-	118.4 s	-
4	172.1 s	-	172.2* s	-
5	104.1 d	6.22 (s)	104.1 d	6.22^{z} (d)
6	168.6 s	-	168.6 s	-
6a	101.2 s	-	101.1 s	-
6b	138.3 s	-	138.3$^{\#}$ s	-
6c	127.7 s	-	127.1 s	-
7	182.9 s	-	183.0 s	-
7a	117.2 s	-	117.9 s	-
8	159.3 s	-	159.3 s	-
9	112.3 d	6.96 (s)	109.0 d	7.06 (s)
10	141.0 s	-	145.7 s	-
11	127.1 d	7.11 (s)	124.0 d	7.25 (s)
11a	129.3 s	-	129.3 s	-
12	127.1 d	7.11 (s)	127.1 d	7.10 (s)
12a	129.3 s	-	129.3 s	-
13	141.0 s	-	141.5 s	-
14	112.3 d	6.96 (s)	112.3 d	6.94 (s)
15	159.3 s	-	159.3 s	-
15a	117.2 s	-	117.1 s	-
16	182.9 s	-	183.0 s	-
16a	101.2 s	-	101.1 s	-
16b	138.3 s	-	138.4$^{\#}$ s	-
16c	127.7 s	-	127.1 s	-
17	21.5 q	2.09 (3H, s)	62.3 t	4.25 (2H, m)
18	21.5 q	2.09 (3H, s)	21.6 q	2.07 (3H, s)
1-OH	-	ND	-	16.24^{x} (s)
3-OH	-	ND	-	18.51^{y} (s)
4-OH	-	ND	-	18.51^{y} (s)
6-OH	-	ND	-	16.25^{x} (s)
17-OH			-	5.16 (m)
8-OMe	56.0 q	3.93 (3H, s)	55.9 q	3.94 (3H, s)
15-OMe	56.0 q	3.93 (3H, s)	55.9 q	3.93 (3H, s)

ND: Not determined. $^{*,\#, x, y, z}$Interchangeble.

3.2. Bioactivity of Compounds

Cytotoxic activities of the compounds were screened against three human prostate cancer cell lines (LNCaP, PC3, and Du145) and a normal prostate cell line (RPWE-1). Results showed that none of the new compounds had cytotoxic activity (Table 3). Also, two known compounds, namely, carviolin (**3**) and 1-*O*-methylemodin (**9**), did not exhibit activity on cell proliferation which is compatible with literature [22, 23]. The other compounds isolated as isomeric mixtures (**1** and **5**) were found to possess antiproliferative activity (Table 3). While **1** showed cytotoxic activity with IC_{50} values between 26 and 37.6 μM, IC_{50} values of **5** could not be calculated since cell viability was not decreased concentration

dependently (Figure 2A). Also, microscopic images showed the formation of dead cell morphology after treatment with compound **1**, while **5** decreased cell number without precise death (Figure 2B). These data indicated that **5** may be a cytostatic compound that does not kill cells but instead inhibits cell proliferation. To prove this proposition, cell death induction via **1** and **5** was investigated using flow cytometry. Results showed that **1** increased apoptotic cell death ratio in line with staurosporine, a well-known apoptosis inducer. But no cell death was observed in compound **5** treated cells (Figure 3A). Together, our data shows that **5** have cytostatic activity while **1** induces cytotoxicity. Contrary to that, the cytotoxic activity of **5** was reported [24, 25], but those studies were carried out against different cancer cell line types instead of the prostate. A study investigating the effects of 301 oncological compounds in 16 triple-negative breast cancer lines reported that molecules may have cytostatic or cytotoxic effects depending on the cell lines. Therefore, the activity mode of **1** and **5** may vary depending on cell line type [26].

Table 3. IC_{50} values of compounds and extract on prostate cell lines

Compounds	LNCaP	PC3	Du145	RPWE-1
1 (11-methoxycurvularin)	26.7 µM	37.6 µM	24.7 µM	29.6 µM
2	>50 µM	>50 µM	>50 µM	ND
3	>50 µM	>50 µM	>50 µM	>50 µM
4	>50 µM	>50 µM	>50 µM	>50 µM
5 (11-hydroxycurvularin)	NC	NC	NC	NC
6	>50 µM	>50 µM	>50 µM	>50 µM
7	>50 µM	>50 µM	>50 µM	>50 µM
8	>50 µM	>50 µM	>50 µM	>50 µM
9	>50 µM	>50 µM	>50 µM	>50 µM
Extract	15 µg/mL	29.5 µg/mL	> 32 µg/mL	ND

ND: not determined, NC: cannot be calculated.

Lastly, we investigated the effect of compounds on the cell cycle by PI staining (Figure 3B). 25 µM of compound **1** was found to decrease the percentage of cells in the G1 and S phases and increase the G2 phase compared to the vehicle (Figure 3C). However, 50 µM of **1** did not affect G2 but arrested cells in G1 with a reduction in the S phase. While an increase in G1 (61.11 % to 77.18 %) and G2 (10.96 % to 15.63 %) populations was observed in 25 µM concentration of compound **5** treated cells, 50 µM concentration of **5** arrested LNCaP cells in G2. These data indicate that compounds **1** and **5** influence the cell cycle differently (Figure 3C). To the best of our knowledge, this is the first report of curvularin-type compounds that inhibit the cell cycle.

Our findings suggested that despite minor structural differences between **1** and **5**, their activity mechanisms were different. Similarly, α,β-dehydrocurvularin, and curvularin were reported to have cytotoxic activity against different cell lines, and only α,β-dehydrocurvularin had superoxide anion scavenging activity [27]. A study examining the activity of many natural and synthetic compounds showed that dehydrocurvularin induced a heat shock response, while curvularin did not [28]. Another report showing the cytotoxic activity of curvularin derivatives on sea urchin embryogenesis revealed that curvularin and 8-dehydrocurvularin affected mitotic spindles, while 8-methoxycurvularin and 8-hydroxycurvularin did not act as spindle poisons and had a different mechanism of action [29]. These data prove that small changes in the structures of curvularin-type molecules may lead to variations in their molecular mechanism.

Although it has been reported that there are similarities in the molecular mechanism of cytostatic and cytotoxic molecules, a study using *in silico* MoA analysis protocol has shown several differences, such as the response to DNA damage, melanin biosynthesis, metabolism, and cytoskeletal mechanisms [30]. Therefore, the difference in activity mechanism between **1** and **5** may arise from the induction of the above-mentioned cell pathways.

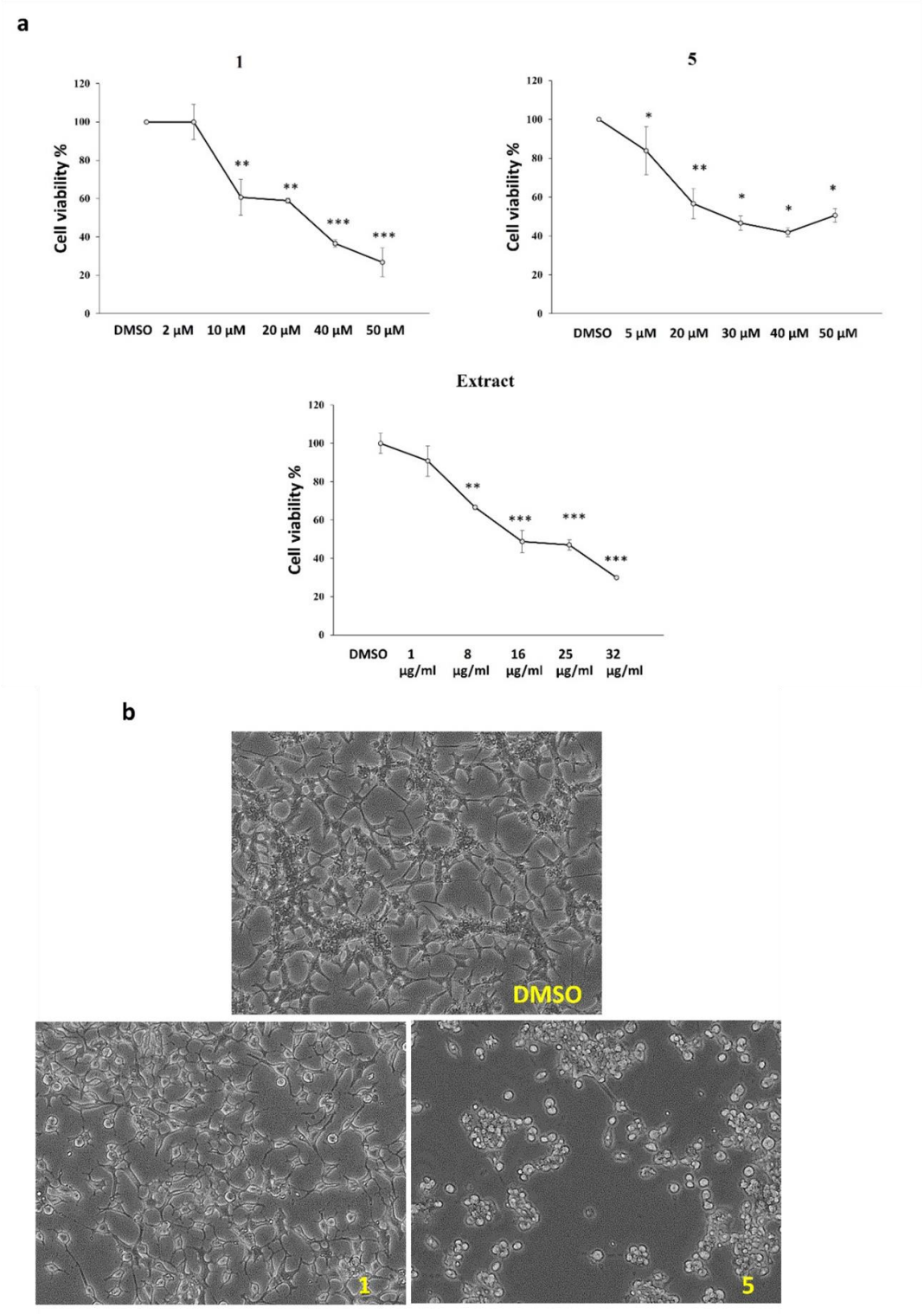

Figure 2. Compounds **1** and **5** affect cell proliferation. (a) After LNCaP cells were treated with various concentrations of compounds/extract, cell viability was determined using MTT assay. (*p<0.05, **p<0.01, ***p<0.001) (b) Microscopic images of LNCaP cells treated with 50 µM of **1** and **5**.

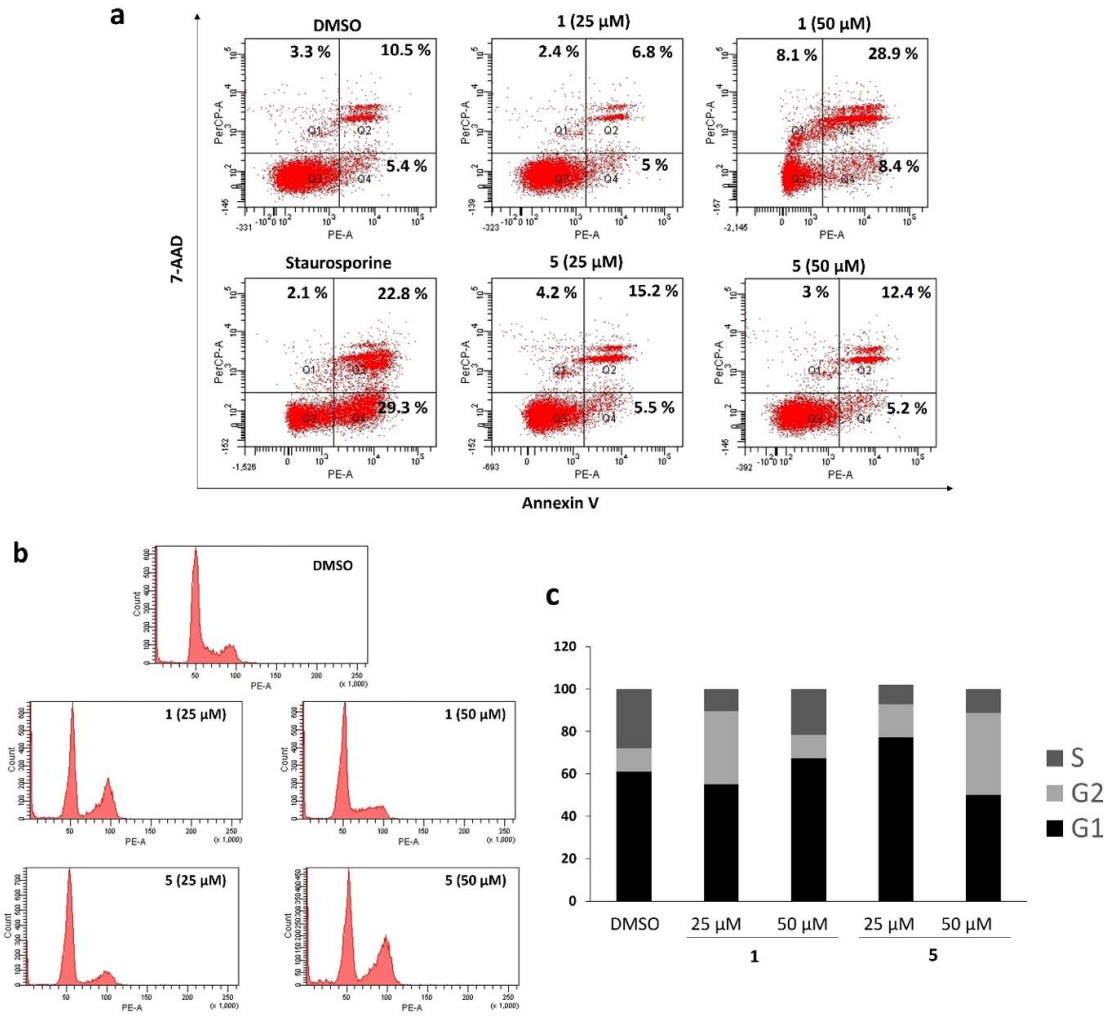

Figure 3. Compounds **1** and **5** affect LNCaP cells differently. (a) LNCaP cells were stained by Annexin V/7-AAD and analyzed via flow cytometry after treatment with compounds for 48 h. Staurosporine (1 µM) was used as an apoptotic inducer. (b-c) Following treatment with compounds for 48 h, cells were stained by PI and analyzed via flow cytometry. (b) Flow cytometry histogram of PI staining. (c) Bar graph showing the percentage of LNCaP cells in the cell cycle phases.

In the current study, five new metabolites were isolated from endophytic fungi *P. roseopurpureum*. Cytotoxicity activity assays showed that only known isolates (**1** and **5**) affect prostate cancer cell proliferation. Interestingly, their activity mechanism differed in LNCaP cells even though their structures are highly similar. Firstly, **1** exhibited cytotoxic activity, while **5** were found to be cytostatic. Secondly, both compounds triggered cell cycle arrest, but at different stages. Those data imply that either the compounds target different site(s)/pathway(s) or their physicochemical character changes, affecting their solubility, cell membrane penetration, distribution, or metabolization properties. However, detailed studies are required to understand the reason for the difference in the mechanism of action of **1** and **5**. Collectively, our study proved that endophytic fungi have a high potential to provide novel natural products with interesting biological activities.

Acknowledgments

We are very grateful to the Pharmaceutical Sciences Research Centre (FABAL, Ege University, Faculty of Pharmacy) and Biotechnology and Bioengineering Application Research Centre (BIYOMER, İzmir Institute of Technology) for equipment support.

Supporting Information

Supporting information accompanies this paper on http://www.acgpubs.org/journal/records-of-natural-products

ORCID
Berivan Dizmen: 0000-0001-7831-0795
Göklem Üner: 0000-0003-4970-4837
Melis Küçüksolak: 0000-0003-1619-4850
Ahmet C. Gören: 0000-0002-5470-130X
Petek Ballar Kırmızıbayrak: 0000-0002-6189-1818
Erdal Bedir: 0000-0003-1262-063X

References

[1] Y.-K. Zheng, X.-G. Qiao, C.-P. Miao, K. Liu, Y.-W. Chen, L.-H. Xu and L.-X. Zhao (2016). Diversity, distribution and biotechnological potential of endophytic fungi, *Ann. Microbiol*. **66**, 529–542.

[2] M.R. Pimentel, G. Molina, A.P. Dionísio, M.R. Maróstica Junior and G.M. Pastore (2010). The use of endophytes to obtain bioactive compounds and their application in biotransformation process, *Biotechnol. Res. Int*. **2011**, 576286.

[3] S. Kusari, S. Singh and C. Jayabaskaran (2014). Biotechnological potential of plant-associated endophytic fungi: hope versus hype, *Trends Biotechnol*. **32**, 297–303.

[4] H. Nisa, A.N. Kamili, I.A. Nawchoo, S. Shafi, N. Shameem and S.A. Bandh (2015). Fungal endophytes as prolific source of phytochemicals and other bioactive natural products: a review, *Microb. Pathog*. **82**, 50–59.

[5] J. Ludwig-Müller (2015) Plants and endophytes: equal partners in secondary metabolite production? *Biotechnol. Lett*. **37**, 1325–1334.

[6] J. Wen, S.K. Okyere, S. Wang, J. Wang, L. Xie, Y. Ran and Y. Hu (2022). Endophytic fungi: An effective alternative source of plant-derived bioactive compounds for pharmacological studies, *J. Fungi*. **8**(**2**), 205.

[7] H.E. Ortega, D. Torres-Mendoza, Z. Caballero, and E. L. Cubilla-Rios (2021). Structurally uncommon secondary metabolites derived from endophytic fungi, *J. Fungi*. **7**(**7**), 570. doi: 10.3390/jof7070570

[8] A.H. Hashem, M.S. Attia, E.K. Kandil, M.M. Fawzi, A.S. Abdelrahman, M.S. Khader, M.A. Khodaira, A.E. Emam, M.A. Goma and A.M. Abdelaziz (2023). Bioactive compounds and biomedical applications of endophytic fungi: a recent review, *Microb. Cell Fact*. **22**, 107. doi:10.1186/s12934-023-02118-x

[9] A. Gupta, V. Meshram, M. Gupta, S. Goyal, K.A. Qureshi, M. Jaremko and K.K. Shukla (2023). Fungal endophytes: Microfactories of novel bioactive compounds with therapeutic interventions; a comprehensive review on the biotechnological developments in the field of fungal endophytic biology over the last decade, *Biomolecules*. **13**(**7**), 1038. doi: 10.3390/biom13071038

[10] J. S. Cruz, C. A. Silva and L. Hamerski (2020). Natural products from endophytic fungi associated with *Rubiaceae* species, *J. Fungi*. **6**(**3**), 128. doi: 10.3390/jof6030128.

[11] M. Ghannoum, M.C. Arendrup, V.P. Chaturvedi, S.R. Lockhart, T.S. McCormick, S. Chaturvedi, E.L. Berkow, D. Juneja, B. Tarai, N. Azie, D. Angulo and T.J. Walsh (2020). Ibrexafungerp: A novel oral triterpenoid antifungal in development for the treatment of *Candida auris* infections, *Antibiotics* **9**(**9**), 539.

[12] F. Pelaez, A. Cabello, G. Platas, M.T. Díez, A.G. Del Val, A. Basilio, I. Martán, F. Vicente, G.F. Bills, R.A. Giacobbe, R.E. Schwartz, J.C. Onishi, M.S. Meinz, G.K. Abruzzo, A.M. Flattery, L. Kong and M.B. Kurtz (2000). The discovery of enfumafungin, a novel antifungal compound produced by an endophytic *Hormonema* species biological activity and taxonomy of the producing organisms, *Syst. Appl. Microbiol*. **23**(**3**), 333-43.

[13] A.G.T. Niego, C. Lambert, P. Mortimer, N. Thongklang, S. Rapior, M. Grosse, H. Schrey, E. Charria-Girón, A. Walker, K.D. Hyde and M. Stadler (2023). The contribution of fungi to the global economy, *Fungal Divers*. **121**, 95–137.

[14] G. Ekiz (2016). Research on bioactive secondary metabolite profile of *Septofusidium berolinense* and biotransformation of cycloartane type saponins by endophytic fungi, PhD Thesis, Ege University, İzmir, Turkey.

[15] Q. Liang, Y. Sun, B. Yu, X. She and X. Pan (2007). First total syntheses and spectral data corrections of 11-α-methoxycurvularin and 11-β-methoxycurvularin, *J. Org. Chem*. **72**(**25**), 9846–9849.

[16] T.M. Ha, W. Ko, S.J. Lee, Y.C. Kim, J.Y. Son, J.H. Sohn, J.H. Yim and H. Oh (2017). Anti-inflammatory effects of curvularin-type metabolites from a marine-derived fungal strain *Penicillium* sp. SF-5859 in lipopolysaccharide-induced RAW264.7 macrophages, *Mar. Drugs*. **15**(**9**), 282.

[17] J. Zhan, E.M.K. Wijeratne, C.J. Seliga, J. Zhang, E.E. Pierson, L.S. Pierson, H.D. Vanetten and A.A.L. Gunatilaka (2004). A new anthraquinone and cytotoxic curvularins of a *Penicillium* sp. from the rhizosphere of *Fallugia paradoxa* of the Sonoran Desert, *J. Antibiot*. **57**(**5**), 341-344.

[18] A.H. Elbanna, Z.G. Khalil, P. V. Bernhardt and R.J. Capon (2021). Neobulgarones revisited: Anti and syn bianthrones from an Australian mud dauber wasp nest-associated fungus, *Penicillium* sp. CMB-MD22, *J. Nat. Prod*. **84** (**3**), 762–770.

[19] A.H. Aly, A. Debbab, C. Clements, R. Edrada-Ebel, B. Orlikova, M. Diederich, V. Wray, W. Lin and P. Proksch (2011). NF kappa B inhibitors and antitrypanosomal metabolites from endophytic fungus *Penicillium* sp. isolated from *Limonium tubiflorum*, *Bioorg. Med. Chem*. **19**(**1**), 414-21.

[20] H. Greve, P.J. Schupp, E. Eguereva, S. Kehraus, G. Kelter, A. Maier, H.H. Fiebig and G.M. König (2008). Apralactone A and a new stereochemical class of curvularins from the marine fungus *Curvularia* sp., *European J. Org. Chem*. **30**. doi: 10.1002/ejoc.200800522.

[21] W.A. Ayer and L.S. Trifonov (1994). Anthraquinones and a 10-hydroxyanthrone from *Phialophora alba*, *J. Nat. Prod.* **57**, 317–319.

[22] R.S.T. Kamdem, W. Pascal, N. Rehberg, L. van Geelen, S.P. Höfert, T.O. Knedel, C. Janiak, P. Sureechatchaiyan, M.U. Kassack, W. Lin, R. Kalscheuer, Z. Liu and P. Proksch (2018). Metabolites from the endophytic fungus *Cylindrocarpon* sp. isolated from tropical plant *Sapium ellipticum*, *Fitoterapia* **128**, 175-179.

[23] F. Eilbert, H. Anke and O. Sterner (2000). Neobulgarones A~F from cultures of *Neobulgaria pura*, new inhibitors of appressorium formation of *Magnaporthe grisea*, *J. Antibiot*. **53**(**10**), 1123-1129

[24] X. Ye, K. Anjum, T. Song, W. Wang, S. Yu, H. Huang, X.Y. Lian and Z. Zhang (2016). A new curvularin glycoside and its cytotoxic and antibacterial analogues from marine actinomycete *Pseudonocardia* sp. HS7, *Nat. Prod. Res*. **30**(**10**), 1156-1161.

[25] J. He, E.M.K. Wijeratne, B.P. Bashyal, J. Zhan, C.J. Seliga, M.X. Liu, E.E. Pierson, L.S. Pierson, H.D. VanEtten and A.A.L. Gunatilaka (2004). Cytotoxic and other metabolites of *Aspergillus* inhabiting the rhizosphere of Sonoran Desert plants, *J. Nat. Prod*. **67** (**12**), 1985–1991.

[26] P. Gautam, L. Karhinen, A. Szwajda, S.K. Jha, B. Yadav, T. Aittokallio and K. Wennerberg (2016). Identification of selective cytotoxic and synthetic lethal drug responses in triple negative breast cancer cells, *Mol. Cancer*. **15**, 34.doi: 10.1186/s12943-016-0517-3

[27] C.G. Kumar, P. Mongolla, P. Sujitha, J. Joseph, K. Suresh Babu, G. Suresh, K.V.S. Ramakrishna, U. Purushotham, G.N. Sastry and A. Kamal (2013). Metabolite profiling and biological activities of bioactive compounds produced by Chrysosporium lobatum strain BK-3 isolated from Kaziranga National Park, Assam, India, *SpringerPlus*, **2**(**1**), 122. doi: 10.1186/2193-1801-2-122.

[28] S. Santagata, Y.M. Xu, E.M. Kithsiri Wijeratne, R. Kontnik, C. Rooney, C.C. Perley, H. Kwon, J. Clardy, S. Kesari, L. Whitesell, S. Lindquist and A.A.L. Gunatilaka (2012). Using the heat-shock response to discover anticancer compounds that target protein homeostasis, *ACS Chem. Biol*. **7**(**2**), 340-349. doi:10.1021/cb200353m

[29] A. Kobayashi, T. Hino, S. Yata, K. Kawazu, T.J. Itoh and H. Sato (1998). Unique spindle poisons, curvularin and its derivatives, isolated from *Penicillium* species, *Agric Biol Chem*. **52** (**12**), 3119-3123.

[30] L. H. Mervin, Q. Cao, I.P. Barrett, M.A. Firth, D. Murray, L. McWilliams, M. Haddrick, M. Wigglesworth, O. Engkvist and A. Bender (2016). Understanding cytotoxicity and cytostaticity in a high-throughput screening collection, *ACS Chem. Biol.* **11**(**11**), 3007–3023.